Hindawi
Shock and Vibration
Volume 2021, Article ID 6687244, 14 pages
https://doi.org/10.1155/2021/6687244

Research Article

Control of Gob-Side Roadway with Large Mining Height in Inclined Thick Coal Seam: A Case Study

Xie Fuxing [1,2,3]

[1]*Mine Construction Branch, China Coal Research Institute, Beijing 100013, China*
[2]*Beijing China Coal Mine Engineering Co., Ltd., Beijing 100013, China*
[3]*China Petroleum Pipeline Bureau, Langfang 065000, China*

Correspondence should be addressed to Xie Fuxing; 17701351006@126.com

Received 27 December 2020; Revised 6 January 2021; Accepted 26 February 2021; Published 4 March 2021

Academic Editor: Sandro Carbonari

The gob-side roadway of 130205, a large-mining-height working face in the Yangchangwan coal mine, was investigated in terms of the mine pressure law and support technology for large mining heights and narrow coal pillars for mining roadways. The research included field investigations, theoretical analysis, numerical simulation, field tests, and other methods. This paper analyzes the form of movement for overlying rock structure in a gob-side entry with a large mining height and summarizes the stress state and deformation failure characteristics of the surrounding rock. The failure mechanism of the surrounding rock of the gob-side roadway and controllable engineering factors causing deformation were analyzed. FLAC3D numerical simulation software was used to explore the influence law of coal pillar width, working face mining height, and mining intensity on the stability of the surrounding rock of the gob-side roadway. Ensuring the integrity of the coal pillar, improving the coordination of the system, and using asymmetric support structures as the core support concept are proposed. A reasonably designed support scheme for the gob-side roadway of the working face for 130205 was conducted, and a desirable engineering effect was obtained through field practice verification.

1. Introduction

The traditional wide coal pillar not only wastes coal resources but also easily leads to stress concentration and several hidden dangers. The narrow coal pillar can reduce the loss of resources and, with targeted support schemes, can better maintain the stability of the roadway's surrounding rock. Therefore, the layout of the gob-side entry driving with a narrow coal pillar has been gradually popularized and applied to large mining height working faces. Many scholars have conducted considerable research on stability control for the surrounding rock of gob-side roadways. The coal rock strength, coal pillar width, mining influence degree, and support strength had significant influence on the surrounding rock of gob-side roadways [1, 2]. The influence of roadway driving and mining disturbance should be comprehensively considered in coal pillar width [3]. The energy support theory had indicated that reasonable support structure and mode should be able to achieve the energy conversion equilibrium state [4]. The main purpose of support was to ensure the integrity and residual strength of surrounding rock in plastic area [5]. The coal pillar support should be strengthened by controlling the rotation of key rock blocks during the mining period for the gob-side entry [6, 7]. Most of the above studies were based on common coal seam roadways, and research on the control of the surrounding rock of gob-side entries in large mining height working faces of inclined thick coal seams remains scarce. There are still some difficulties in the research of surrounding rock control technology of gob-side entry with large mining height in inclined thick coal seam: (1) The mining space is larger, the movement range of overlying rock is larger, and the influence of high lateral support pressure on the stability of surrounding rock of gob-side entry is more obvious; (2) In the past, the surrounding rock control of gob-side entry is mostly symmetrical control

scheme, and the mining performance of gob-side entry in inclined thick coal seam is asymmetric, so it is necessary to put forward more targeted asymmetric control scheme. Therefore, the research on surrounding rock control technology of gob-side entry with large mining height in inclined thick coal seam has great innovation.

2. Engineering Background

2.1. Engineering Geology. The Yangchangwan coal mine primarily focuses on the No. 2 coal seam. The coal seam has a simple structure, with an average thickness of 7.9 m, an average dip angle of 18°, and well-developed joints. The Proctor coefficient $f = 1\sim2$. The rock properties of the roof and floor of the coal seam are depicted in Figure 1. There is a 0.2–0.6 m thick false roof between the No. 2 coal seam and the direct roof. The false roof is affected by the ground pressure and mining and falls during mining, which makes roof management of the working face difficult. Moreover, because the direct bottom of the No. 2 coal seam is siltstone, it easily softens after encountering water, which leads to severe bottom drilling of support and delays in the normal advance of the working face.

2.2. Engineering Background. The 130205 working face is located in the middle of the first division of the Yangchangwan mine, with a buried depth of 630 m, and the mining method of full thickness with large mining height has been adopted for it. The north side of 130205 working face is the 130203 goaf, and the south side is the 130207 working face. The 130205 return air roadway is adjacent to the 130203 goaf, and the roadway location is depicted in Figure 2. A 5 m coal pillar is reserved for the 130205 return air roadway, which is driven along the roof of the coal seam. The width and height of the roadway excavation are 5 and 4 m, respectively.

In the initial stage of driving along goaf roadway in the 130205 working face of Yangchangwan Coal Mine, the field-measured displacement of two sides of roadway reaches 457 mm, the subsidence of coal pillar side roof is 268 mm, and the subsidence of solid coal side roof is 192 mm. The mine pressure behavior of roadway shows obvious asymmetry.

3. Ground Pressure Behavior Characteristics of Gob-Side Entry

3.1. Overlying Rock Structure of the Gob-Side Entry. Professor Hou Chaojiong put forward the concept of "Large structure" and "Small structure" for overlying rock structure and surrounding rock. "Large structure" refers to the mutual hinged structure formed by the roadway overlying rock after mining at an adjacent working face. "Small structure" refers to the common bearing body formed by surrounding rock and supporting materials [8]. The movement of overlying rock of the large structure will directly affect the stability of small structures.

After the upper section of the working face is mined out, the basic roof of the goaf is broken in an "O-X" shape [9], and an arc triangle block structure is formed along the goaf tendency, as shown in Figure 3. The stability of key block B in the structure will directly affect the deformation and failure degree of the surrounding rock of the gob-side roadway. After the upper working face is mined, the coal and rock in the gob-side roadway area are damaged by mining, and the plastic area mainly concentrates on the side of the narrow coal pillar [10–12]. The disturbance of roadway driving along the goaf is relatively small, and the degree of damage to the surrounding rock is small. The mining influence caused by the current working face mining intensifies the movement of the overlying rock structure and the degree of damage to the roadway's surrounding rock [13]. Therefore, reasonable support mode and strength in the driving stage are decisive factors to ensure current mining safety.

3.2. Stress Characteristics of Surrounding Rock. After the stoping of the upper working face enters the stable period, the internal stress of the rock mass in the area to be arranged gradually enters the equilibrium state [14–16]. When driving along the goaf, the equilibrium state is broken, and the stress of the surrounding rock is redistributed, but the degree of influence is low. The mining influence caused by the current working face mining will aggravate the destruction of the surrounding rock's stability.

There is a certain plastic zone depth in the shallow part of the surrounding rock after roadway excavation. According to the limit strength of the surrounding rock in the area, the stress and displacement distribution around the roadway can be solved by the elastic-plastic limit equilibrium theory [17]. Assuming that the tunnel section is circular, the stress of surrounding rock is analyzed and solved through elastic-plastic theory. The radial stress σ_r^e and circumferential stress σ_θ^e in the elastic zone of the surrounding rock are obtained as follows [18–20]:

$$\sigma_r^e = p_0\left(1-\frac{a^2}{r^2}\right)+\left[c\times ctg\phi\left(\frac{R_P}{a}\right)^{(2\sin\phi/1-\sin\phi)}-c\times ctg\phi\right]\frac{a^2}{r^2},$$

$$\sigma_\theta^e = p_0\left(1+\frac{a^2}{r^2}\right)-\left[c\times ctg\phi\left(\frac{R_P}{a}\right)^{(2\sin\phi/1-\sin\phi)}-c\times ctg\phi\right]\frac{a^2}{r^2}, \tag{1}$$

where C is the cohesion of the surrounding rock, φ is the surrounding rocks' internal friction angle, r is the spacing between the surrounding rock and roadway center, a is the circular section roadway radius, and P_0 is the original rock stress.

The radial stress σ_r^p, circumferential stress σ_θ^p, and radius R_P of the plastic zone of the surrounding rock are, respectively, as follows [21–23]:

$$\sigma_r^p = c\times ctg\phi\left[\left(\frac{r}{a}\right)^{(2\sin\phi/1-\sin\phi)}-1\right],$$

$$\sigma_\theta^p = c\times ctg\phi\left[\frac{1+\sin\phi}{1-\sin\phi}\left(\frac{r}{a}\right)^{(2\sin\phi/1-\sin\phi)}-1\right], \tag{2}$$

$$R_P = a\left[\frac{(p_0+c\times ctg\phi)(1-\sin\phi)}{c\times ctg\phi}\right]^{(1-\sin\phi/2\sin\phi)}\frac{1}{2}.$$

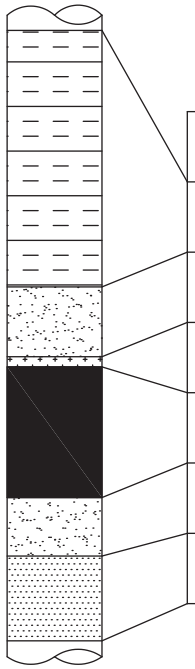

Rock stratum	Rock character	Thickness/m	Features
Main roof	Sandstone	15.6 m	Good integrity
Immediate roof	Siltstone	3.9 m	Joint and fissure development
False roof	Mudstone	0.8 m	Bedding development
2# coal seam	Coal	7.9 m	Structure is simple, joints are developed
Immediate floor	Siltstone	3.5 m	Less bedding
Main floor	Fine sandstone	5.1 m	Good integrity

Figure 1: Rock property characteristics of the coal seam roof and floor.

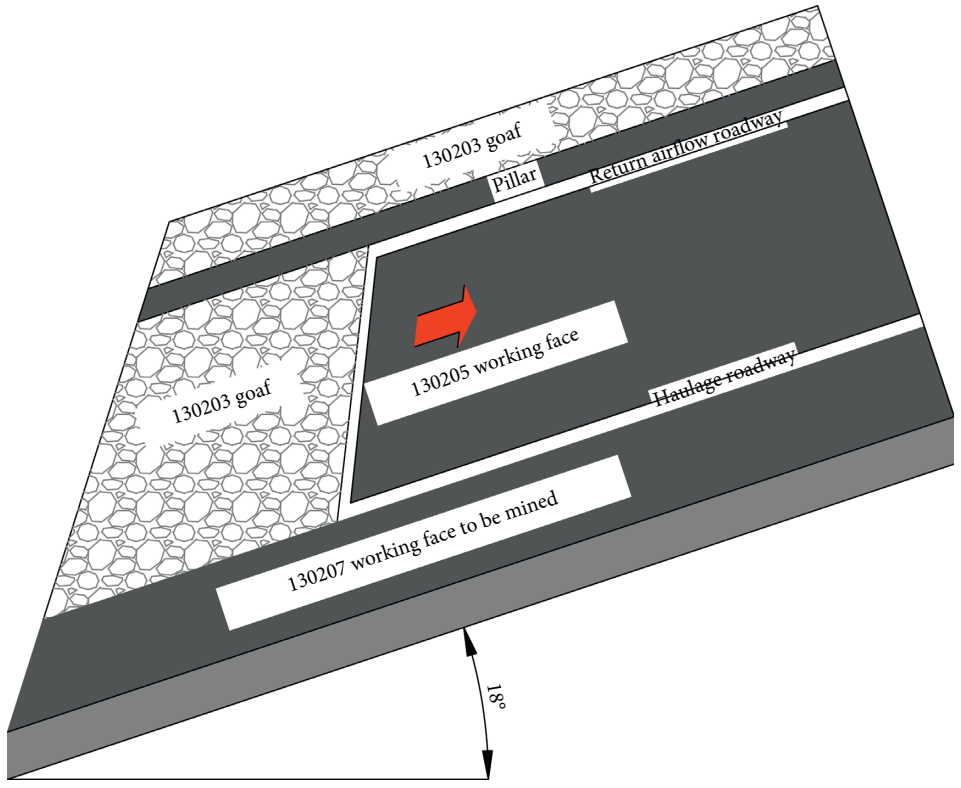

Figure 2: Schematic diagram of roadway location.

Therefore, the stress distribution characteristics of surrounding rock are closely related to the roadway radius, the cohesion of rock mass, the internal friction angle of the rock mass, and the original rock stress. With the increase of mining depth, the original rock stress γH also increases. Furthermore, the surrounding rock stress and the range of the plastic zone also increase correspondingly. There is a positive correlation between the depth of the plastic zone and the size of the roadway section [24]. When the roadway section is fixed, the farther the plastic zone is from the

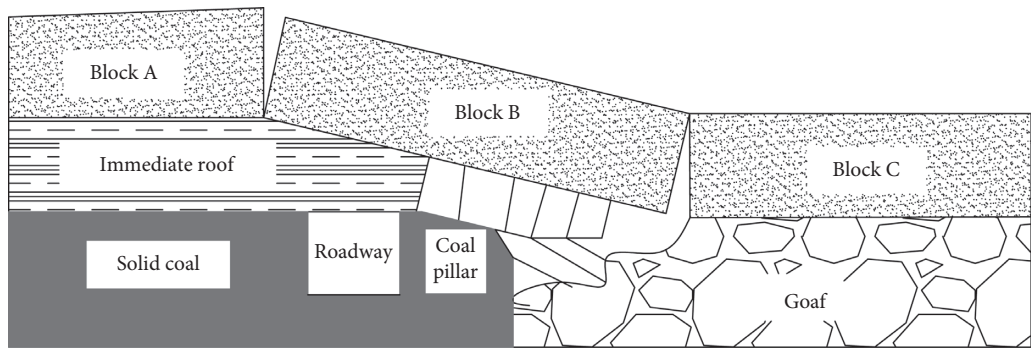

Figure 3: Overlying rock structure of gob-side entry.

roadway center line, the greater the surrounding rock stress. Moreover, the support resistance has a positive correlation with the stress and range in the plastic zone.

From the overburden structure and stress distribution characteristics of gob-side entry, it can be seen that the roof structure of gob-side entry presents obvious asymmetry, and the key triangle structure of the roof has more direct influence on the stress and displacement of coal pillar side of entry, which is consistent with the field-measured value at the initial stage of entry driving.

4. Failure Mechanism of the Surrounding Rock in Gob-Side Entry

4.1. Failure Mode of Surrounding Rock

(1) *Compression-Shear Failure.* Compression-shear failure often occurs on the sides of roadways [25]. The shallow surrounding rocks of the sides are in a plastic state, and spalling and sliding along the shear section due to the influence of vertical stress occur easily.

(2) *Tensile Failure*. Generally, the tensile strength of the surrounding rock is far lower than its compressive strength, and tensile failure occurs when the tensile stress of the rock mass is greater than its tensile strength [24].

(3) *Multiple-Shear Failure*. Multiple-shear failure refers to the shear failure of the rock mass along different weak planes [26]. However, the shear stress at failure does not reach the shear strength of the rock mass. This kind of failure mode mainly occurs in rock masses with high strength and developed joints.

Due to the complex stress environment of the surrounding rock of the narrow pillar of the mining roadway and the development of roof joints in 130205 working face, two or more types of composite failure occur frequently.

4.2. Failure Mechanism of Surrounding Rock. Due to the development of joints and fissures and low strength in the surrounding rock of the roadway, the stress of the surrounding rock exceeds its own strength after repeated mining and the state changes from elasticity to plasticity [27, 28]. The shallow surrounding rock of the roadway is in a two-way stress state, which will gradually cause a chain reaction of deep surrounding rock failure and constant change to a plastic state. During roadway excavation, the roof rock of the roadway evolves from quadrilateral-embedded support to beam-type restraint support and the load generated by the strata above the roadway transfers to the side. The plastic state appears in the restrained section of the two sides. Furthermore, the actual constraint transfers to the interior of the surrounding rock, and the stress in the roof decreases in a negative exponential curve [29]. In this process, the fracture and plastic zones of the surrounding rock are formed and expanded, and the elastic zone transfers to the deep coal body [30]. The support capacity of the plastic zone and the cataclastic zone of the surrounding rock decrease, and the vertical stress transfers to the surrounding rock and forms the stress concentration area. The stress state of surrounding rock is similar to that driving along the goaf, but the mining influence becomes more severe.

5. Influencing Factors of Surrounding Rock Stability

The stability of surrounding rock in a gob-side entry with large mining height is affected by several factors, among which the main engineering influencing factors include coal pillar width, coal seam mining height, and mining influence. Based on the Mohr–Coulomb constitutive relation [31, 32], the numerical model is established with *FLAC3D*. The calculation model is 200 m long, 100 m wide, and 50 m high, as depicted in Figure 4. The Mohr–Coulomb model is adopted for the constitutive relationship of the surrounding rock. The upper boundary of the model is a free surface, and the overburden load of 630m depth is 15.44 MPa; the other five surfaces of the model are fixed boundaries, and the displacement and velocity are set to zero. When the overburden load is applied on the top of the model, the load generated by the overburden at the height of 30m above the top of the model coal seam should be deducted. For the change of coal seam dip angle, the height of the model changes with the dip angle and the load subtracted changes in the same proportion. To obtain the distribution characteristics of stress and displacement of surrounding rock in a gob-side entry, measuring lines are arranged on both sides of

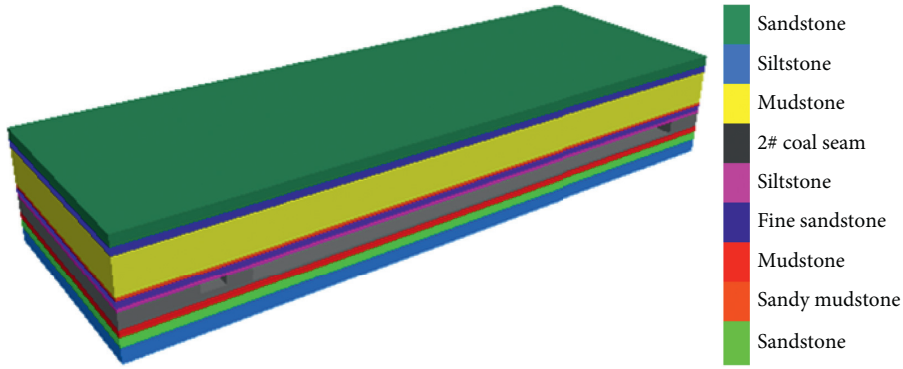

Figure 4: Numerical calculation model.

the roadway and on its roof at 0.5 m intervals, and they are used to analyze the quantitative relationship between various factors and the stability of the gob-side entry's surrounding rock.

5.1. Influence of Coal Pillar Width on the Stability of Surrounding Rock. The width of the coal pillar directly affects the distribution of lateral abutment pressure and has a direct correlation with the stability of the surrounding rock of the roadway along a goaf [33, 34]. Six coal pillar widths (i.e., 3 m, 5 m, 8 m, 12 m, 20 m, and 30 m) were selected to simulate and analyze the stress distribution state of the gob-side roadway.

5.1.1. Stress Distribution of Surrounding Rock with Different Coal Pillar Widths. (1). Stress Distribution of the Roof. The vertical stress distribution of the surrounding rock of roadways with different pillar widths is shown in Figure 5. When the width of the coal pillar is less than 8 m, the peak value of lateral abutment pressure is located at the side of the solid coal. When the width of the coal pillar is greater than 12 m, the peak value of stress is in the coal pillar, and with the increase of coal pillar width, the phenomenon of stress concentration in the coal pillar becomes more obvious. When the width of the coal pillar is less than 12 m, the vertical stress distribution is asymmetric, and the smaller the width of coal pillar, the more obvious the asymmetry of stress distribution. When the width of the coal pillar is less than 5 m, the vertical stress of the shallow surrounding rock at the solid coal side is significantly greater than that at the coal pillar side. Moreover, the lateral abutment pressure is transferred to the deep part of the solid coal, and the roof-breaking range of the coal pillar side is larger and the stress value is smaller.

(2) Stress Distribution of Two Sides. It can be seen from Figure 5 that the vertical stress of the solid coal side decreases with the increase of the coal pillar width and that the vertical stress of the coal pillar side increases with the increase of the coal pillar width. Furthermore, the degree of stress concentration of the solid coal side increases with the decrease of coal pillar width, and the peak position moves inward. When the width of coal pillar is less than 5 m, the coal pillar is basically in plastic state and the stress is less than the original rock stress. When the width of the coal pillar is more than 5 m, there is a stress-rising area in the coal pillar, and the stress concentration coefficient increases with the increase in coal pillar width. When the width of the coal pillar is less than 8 m, the vertical stress of the solid coal side is significantly greater than that of coal pillar side, whereas when the width is more than 8 m, the vertical stress of the solid coal side is larger than that of the solid coal wall.

5.1.2. Displacement Characteristics of Surrounding Rock under Different Coal Pillars of Varying Width. (1) Roof Displacement. The vertical displacement distribution of the roadway roof with coal pillars of varying width is depicted in Figure 6. Changes in coal pillar width have a significant impact on the vertical roof subsidence of the coal pillar roadway. When the width of the coal pillar is less than 20 m, the roof subsidence shows obvious asymmetry. The roof subsidence at the side of the coal pillar is greater than that at the solid coal side. In particular, when the width of the coal pillar is 12 m, the range of the roadway's roof subsidence exceeds 100 mm. When the width of coal pillar is more than 20 m, roof subsidence decreases obviously. When the width of the coal pillar is 3 m, the roof subsidence is smaller than that of 5 m, 8 m, and 12 m coal pillars, which indicates that roadway protection with narrow coal pillars can also be located in low-stress areas.

(2). Displacement of Two Sides. The displacement of two sides of the roadway is depicted in Figure 7. The change in coal pillar width has a particularly significant impact on the horizontal displacement of both sides of the gob-side roadway. When the width of the coal pillar is less than 20 m, the horizontal displacement of the solid coal side is obviously greater than that of coal pillar side, and the maximum displacement can reach twice that of the coal pillar side. With the increase in coal pillar width, the zero horizontal displacement line in the coal pillar gradually transits from the solid coal side to the goaf side.

5.2. Influence of Mining Height on Surrounding Rock Stability. Mining height is also an important parameter affecting the stability of surrounding rock in a gob-side entry. Various mining heights affect the degree of influence of goaf collapse on surrounding rock stability [9]. The distribution law of stress and displacement of surrounding rock in a gob-side entry under six mining height schemes of 2 m, 3 m, 4 m, 5 m, 6 m, and 7 m is simulated and analyzed.

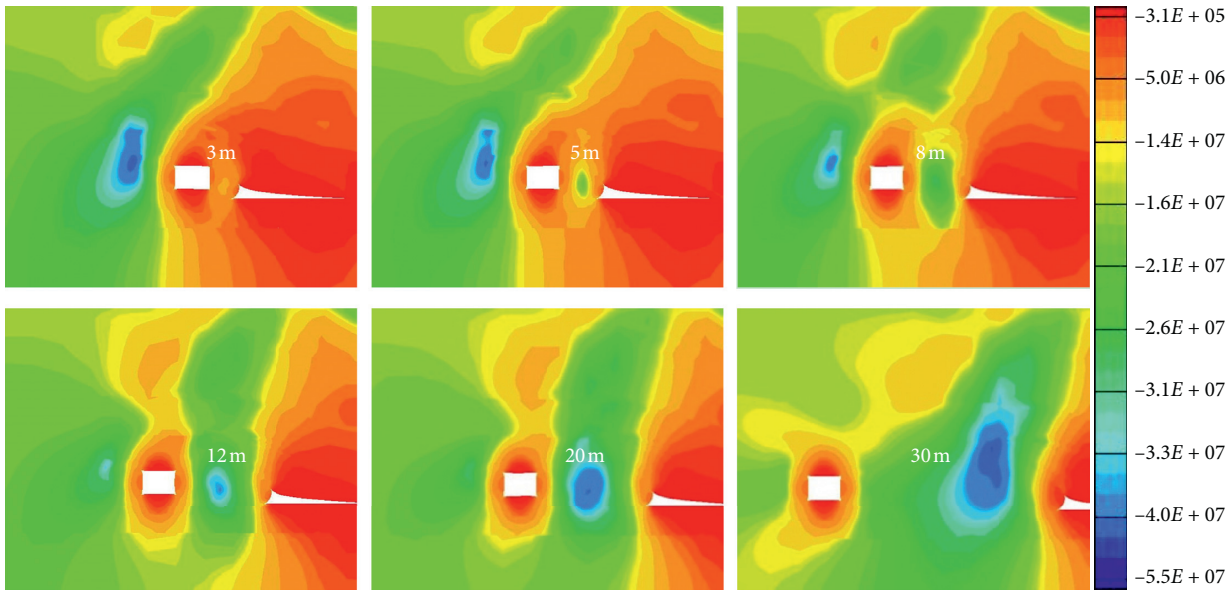

Figure 5: Vertical stress distribution under different coal pillar widths.

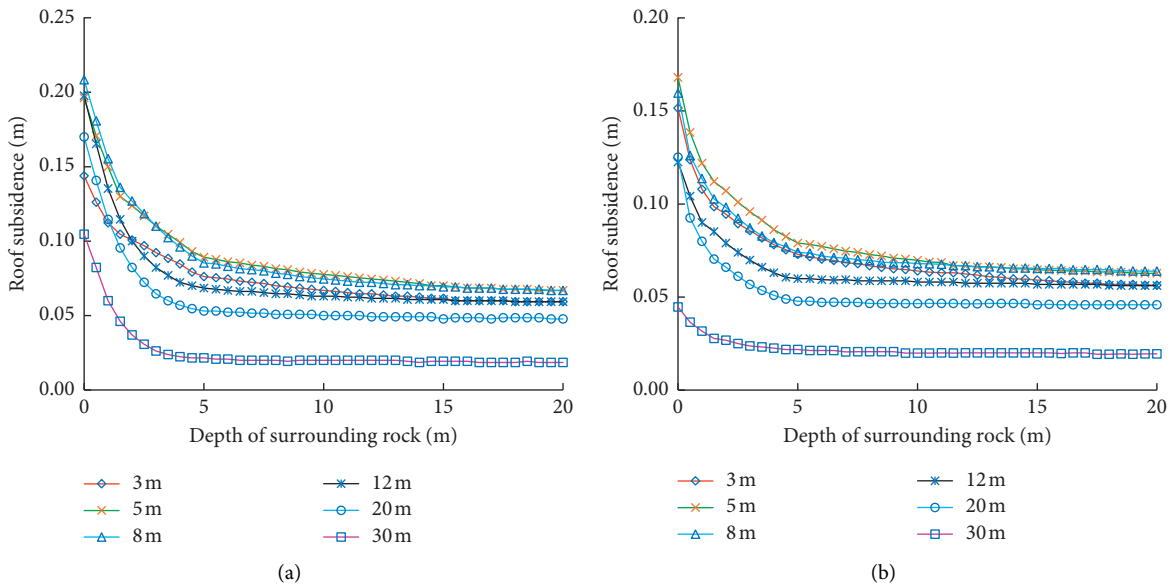

Figure 6: Vertical displacement distribution of roof under different coal pillar widths: (a) coal pillar side roof; (b) solid coal side roof.

5.2.1. Stress Distribution of Surrounding Rock with Different Mining Heights. (1) Stress Distribution of the Roof. The vertical stress distribution of surrounding rock with different mining heights is depicted in Figure 8. When the mining height is less than 4 m, the vertical stress at the coal pillar side is slightly greater than that at the solid side within a roof depth of 0–4 m. However, with the increase in mining height, the difference between the vertical stress at the solid side and the coal pillar side gradually increases. The vertical stress of the solid coal side is greater than that of the coal pillar side within a depth range of 4–13 m, and the difference between the two sides is prominent with the increase in mining height. When the depth is more than 15 m, the vertical stress of the coal pillar side is greater than that of the solid side, and the difference decreases with the increase in mining height. The results show that the larger the mining height, the more serious the damage to the roof of the coal pillar from lateral abutment pressure, whereas the vertical stress of the solid coal side changes little.

(2) Stress Distribution of Two Sides. The vertical stress within 0–5 m of the solid coal wall increases rapidly with the increase in the depth of surrounding rock, and the difference of stress value under different mining height is not obvious. When the depth of surrounding rock is greater than 5 m, the vertical stress decreases with the increase in mining height.

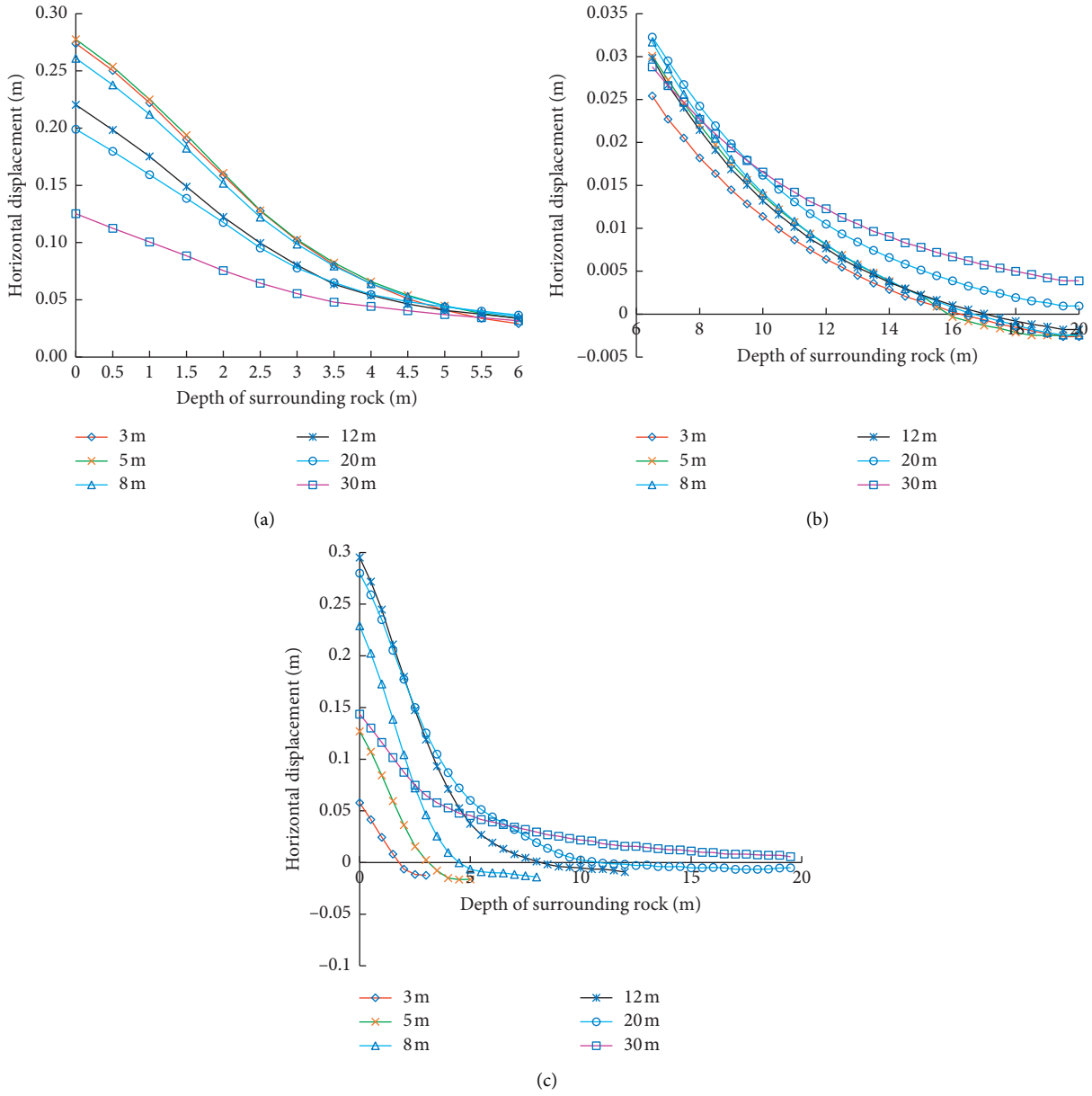

FIGURE 7: Horizontal displacement of (a) shallow surrounding rock in the solid coal wall, (b) deep surrounding rock in the solid coal wall, and (c) coal pillar side.

Within the range of 0–2 m, the vertical stress increases gradually; within the range of 2–5 m, the stress concentration phenomenon appears, and the stress concentration coefficient decreases with the increase in mining height.

The vertical stress in the solid wall rock is larger than that in the coal pillar wall rock, and the larger the mining height, the greater the difference. Such a relationship shows that the peak value of lateral abutment pressure of the surrounding rock in the gob-side entry is transferred to the solid coal side.

5.2.2. Displacement Characteristics of Surrounding Rock with Different Mining Heights. Results reveal that the vertical displacement of the roof is less affected by the mining height but that the horizontal displacement of the two sides is asymmetric.

It can be seen from Figure 9 that the subsidence on both sides of the roof decreases with the increase in mining height. The vertical displacement of the coal pillar side roof is obviously larger than that of the solid side roof, and it is more obvious in depths ranging from 0 to 5 m for the surrounding rock.

It can be seen from Figure 10 that the horizontal displacement of the coal pillar side decreases with the increase in mining height, and the horizontal displacement of the solid side is not affected by the change in mining height.

5.3. Influence of Mining on Surrounding Rock. The influence of mining includes the direct inducement of large-scale

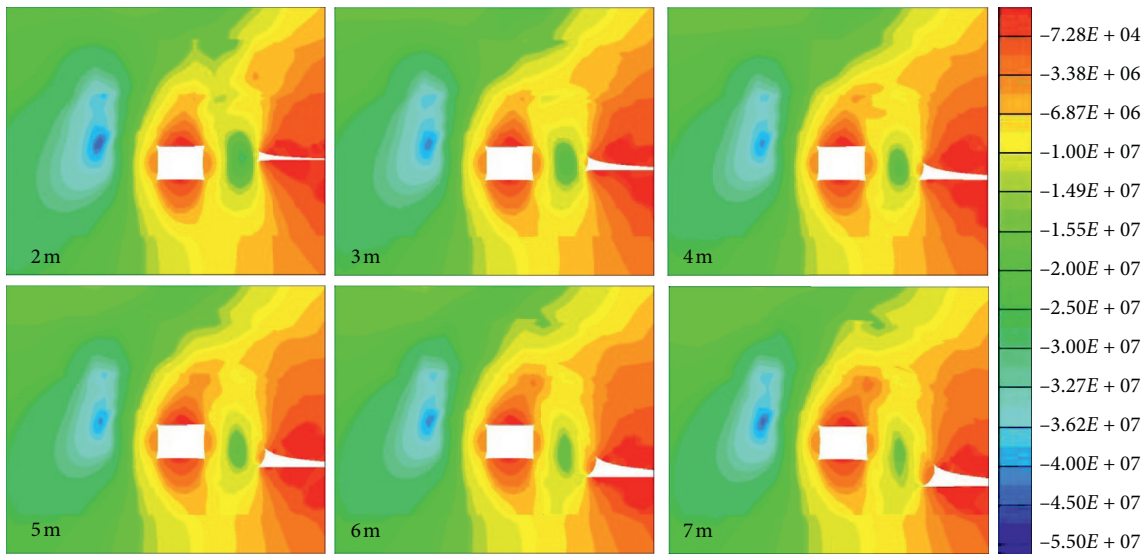

Figure 8: Vertical stress distribution of surrounding rock with different mining heights.

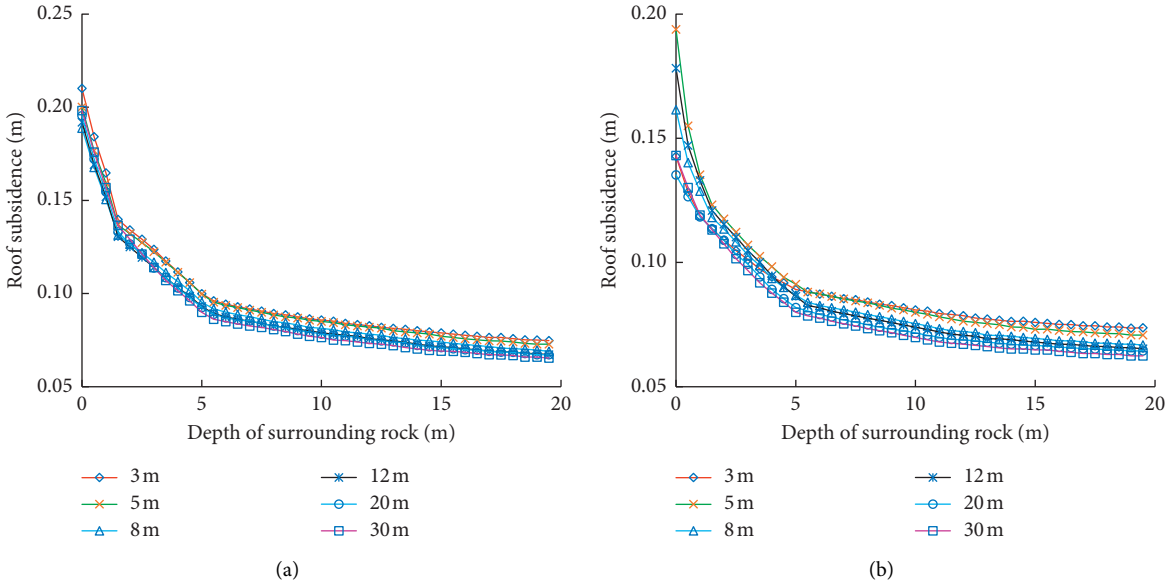

Figure 9: Vertical displacement of the roadway roof at different mining heights: (a) coal pillar side roof; (b) solid coal side roof.

damage to the surrounding rock of roadways [10, 11]. The evolution law of stress and displacement for the surrounding rock of roadways under different mining distances is simulated and analyzed, and the difference of stress and deformation of the surrounding rock of a roadway along the goaf under dynamic and static pressure environments is compared.

5.3.1. Stress Distribution of Surrounding Rock Affected by Mining. Figure 11 shows the vertical stress distribution in the surrounding rock of a roadway before mining (static pressure) and during mining (dynamic pressure).

(1) The variation trend of the roof vertical stress in terms of the depth of the surrounding rock remains the same before and during mining, but the roof gap of the solid coal side is obviously smaller than that of the coal pillar side, which indicates that mining has a stronger influence on the roof of the coal pillar side, which increases the stress asymmetry of the roof. Vertical stress within depths ranging from 0 to 5 m in the roof of the coal pillar side displays a downward trend, which indicates that this part of the rock mass is severely damaged, which is obviously smaller than that of the solid side. Roof asymmetry within the range of 5–10 m is especially obvious, which indicates that the "large structure" of the roof has a certain supporting effect on the side overburden of the coal pillar.

(2) The vertical stress in the solid coal wall decreases with the weakening of mining influence, and the

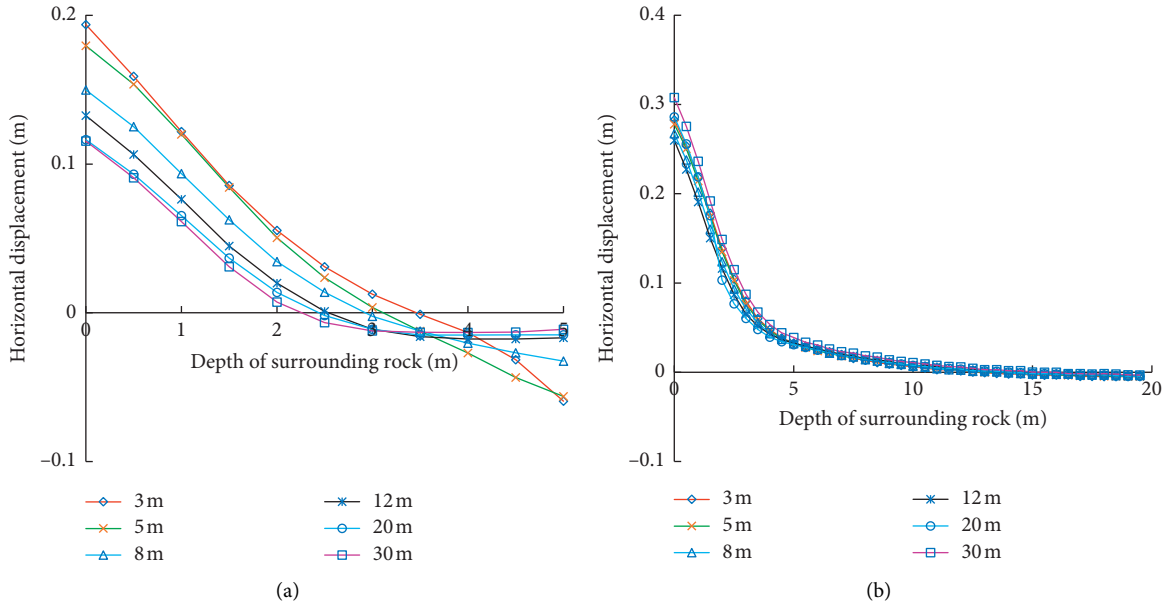

Figure 10: Horizontal displacement of two sides in a roadway at different mining heights: (a) coal pillar side; (b) solid coal side.

peak position shifts to the roadway. The vertical stress in the coal pillar side changes little with mining influence. The difference between the peak value of vertical stress in the solid side wall and that in the coal pillar side increases with the increase in the degree of mining influence, and the maximum value triples. The more severe the mining effect, the more obvious the asymmetry of the two sides.

5.3.2. Displacement of Surrounding Rock under Dynamic Pressure. Figure 12 shows the distribution of subsidence on both sides of the roof under different degrees of mining influence. The analysis shows that subsidence regularity on both sides of the roof is consistent and strong. With the deepening of mining influence degree, roof subsidence increases, and the subsidence of the shallow surrounding rock on the solid side of the roof is large.

Figure 13 depicts the horizontal displacement distribution of surrounding rock within a 0–5 m depth in both sides of the roadway under different degrees of mining influence. The analysis reveals that the horizontal displacement of the solid coal slope increases with the increase in mining intensity and that the shallow part of coal slope is more significant. In the coal pillar side, the level of surrounding rock at a depth of 0–2 m is negative moving to the roadway, and the displacement value within a 2–5 m depth is positive moving to the goaf side. In shallow surrounding rock (0–2 m), the horizontal displacement of the solid side is obviously larger than that of the coal pillar side (almost twice the size).

6. Control Measures of Surrounding Rock in Gob-Side Entry

6.1. Key Points for Surrounding Rock Control in a Gob-Side Entry. Based on the above research, the key points of surrounding rock control of a gob-side entry in an inclined coal seam are proposed as follows:

(1) *Improving Coal Pillar Integrity*. Some deformation of the coal pillar is allowed, but its integrity is maintained [35]. The integrity of the coal pillar should be maintained, while avoiding the chain reaction failure of the roadway's surrounding rock.

(2) *Improving the Coordination of Support Systems* [36]. Key to surrounding rock control is improving the coordination and integrity of the support system, promoting the surrounding rock and support structure to form a common bearing body, and advancing the overall bearing capacity of the surrounding rock.

(3) *Asymmetric Supporting Structure Should Be Adopted*. The asymmetry of surrounding rock bearing in a gob-side entry is obvious, and with the decrease in coal pillar width and the coal seam dip angle, along with other factors, asymmetry is intensified [37, 38]. The targeted asymmetric support structure can better control the deformation of surrounding rock.

6.2. Surrounding Rock Control Scheme of Gob-Side Entry. The surrounding rock of the gob-side entry with large mining height in the Yangchangwan mine is severely damaged. The stress environment is changeable in different stages, and the stress and displacement distribution of the surrounding rock are asymmetric. Therefore, the asymmetrical layout of the supporting structure was adopted. The coupling control scheme of "prestressed anchor cable-+anchor bolt+mesh+shotcreting" was adopted for the gob-side roadway of the 130205 working face, as shown in Figure 14.

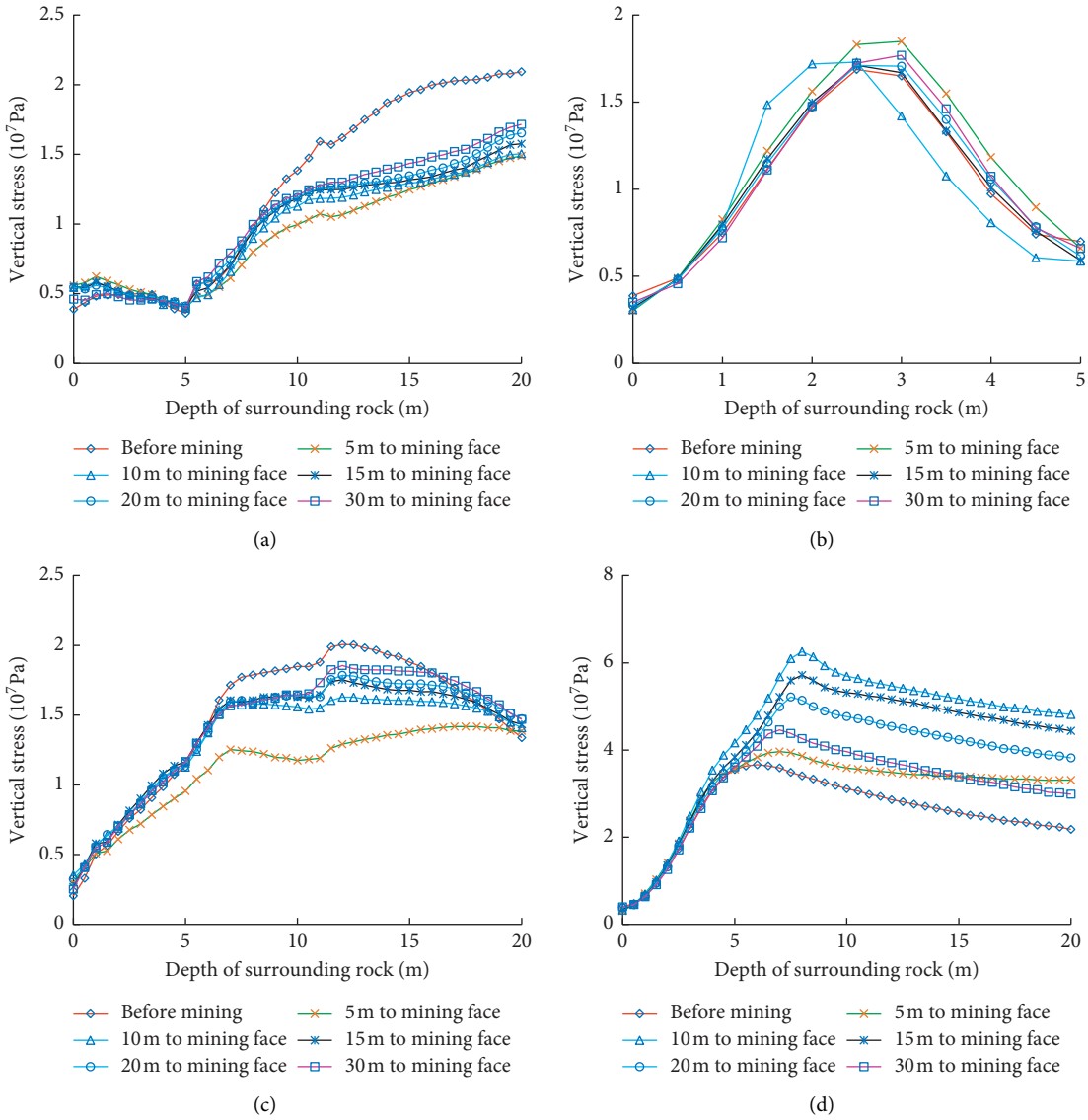

Figure 11: Vertical stress of surrounding rock under different mining conditions: (a) coal pillar side roof; (b) coal pillar side; (c) solid coal side roof; (d) solid coal side.

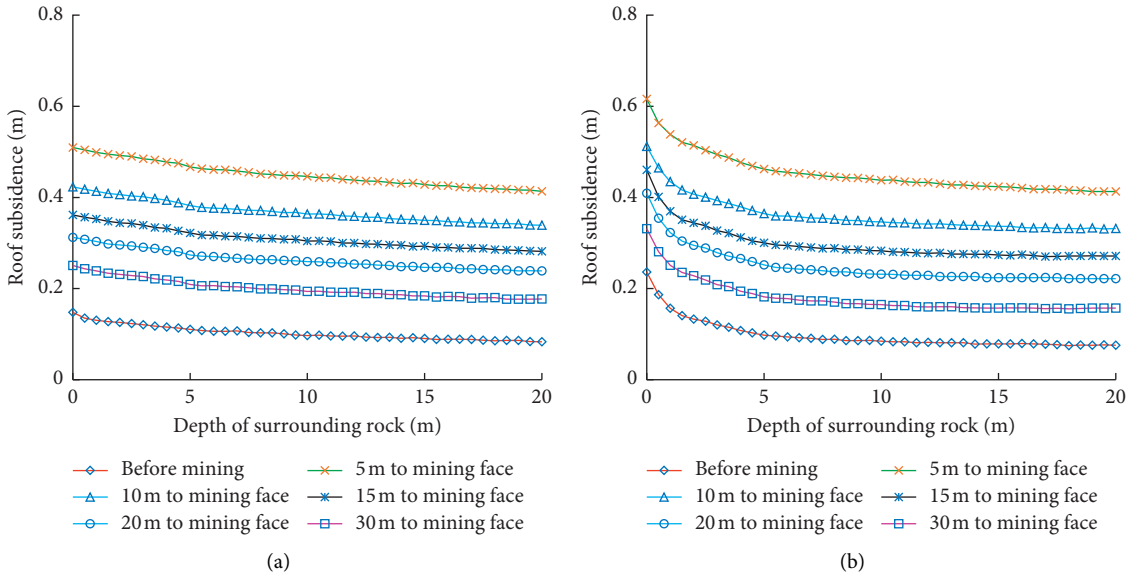

Figure 12: Vertical displacement of the roof: (a) coal pillar side roof; (b) solid coal side roof.

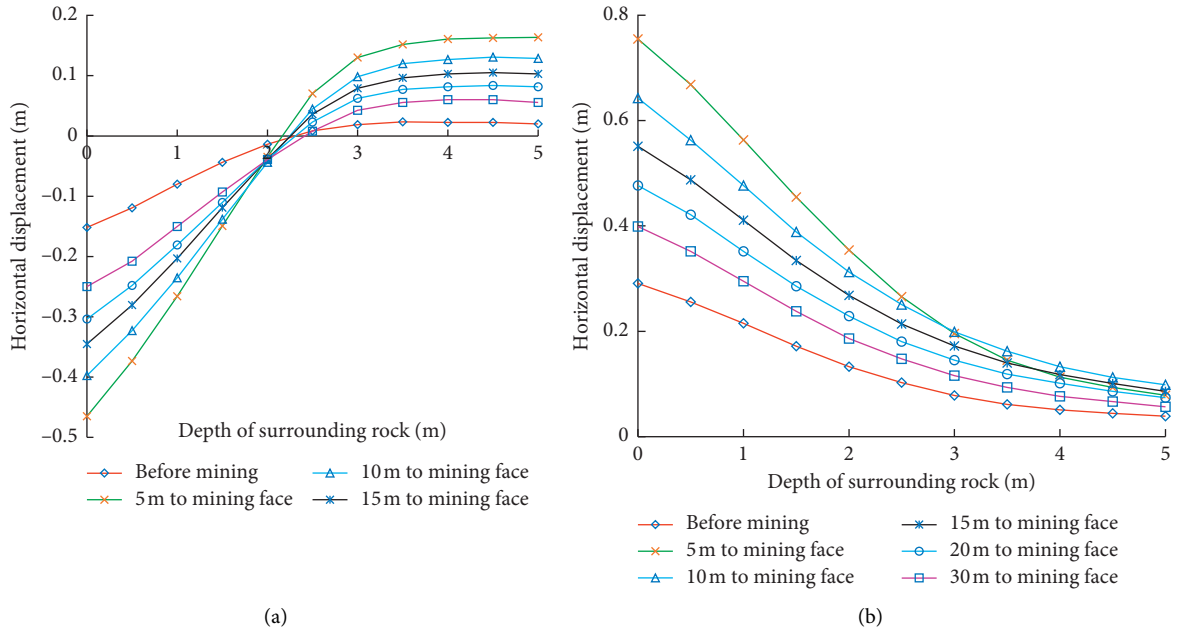

Figure 13: Horizontal displacement of two sides under different mining intensities: (a) coal pillar side roof, (b) solid coal side roof.

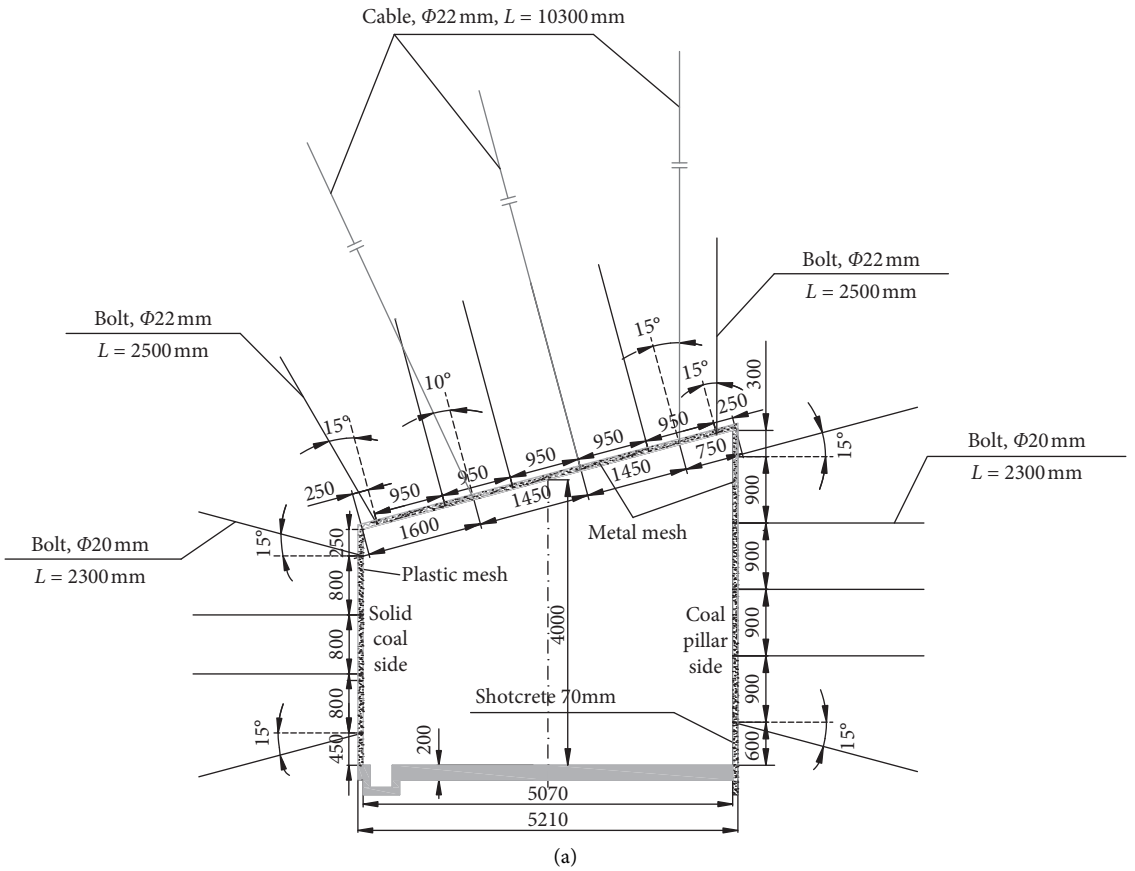

Figure 14: Continued.

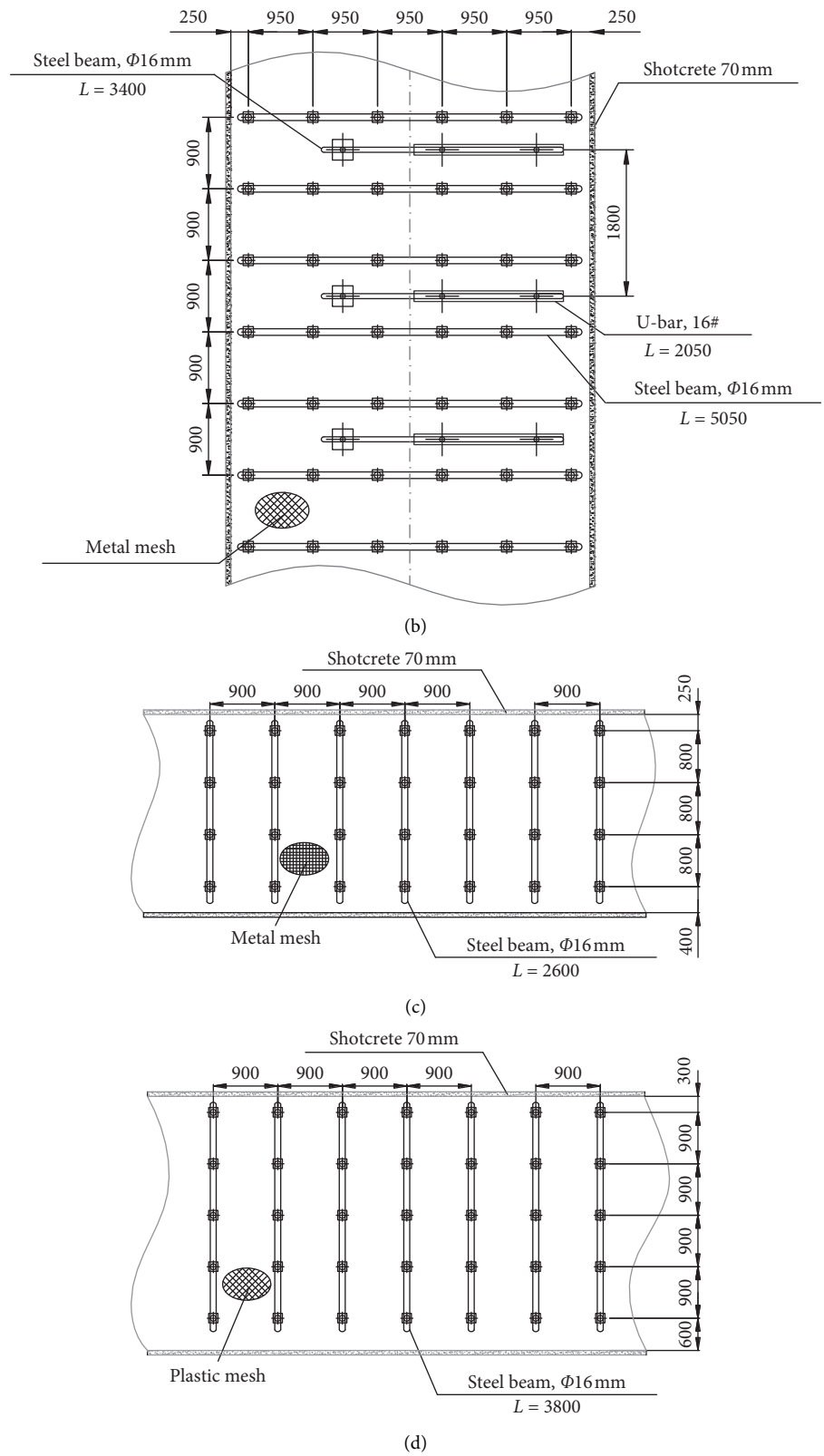

Figure 14: Surrounding rock control scheme of gob-side entry: (a) cross section of roadway support; (b) top view of roof support; (c) front view of coal pillar side support; (d) front view of solid coal side support.

6.3. Control Effect of the Surrounding Rock. During the roadway excavation, the roof subsidence of the side of the solid coal side lasted for 2 months and began to stabilize on the 25th day. The displacement results of surrounding rock surface are shown in Figure 15. During the mining period for 130205s working face, the maximum surface displacement of

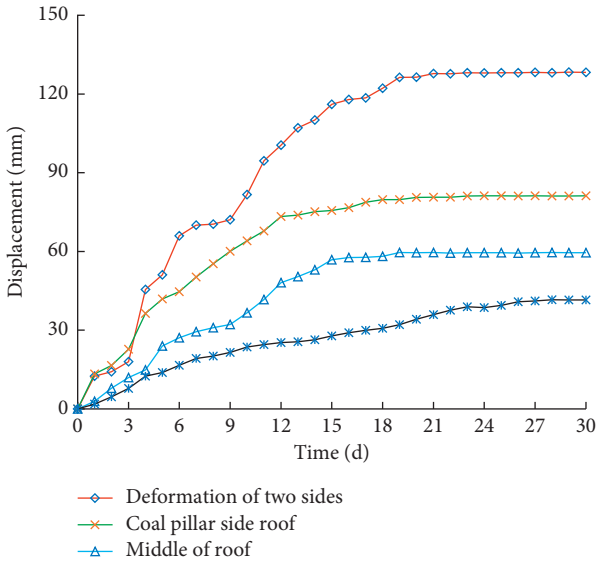

Figure 15: Surface displacement monitoring results.

Figure 16: Control effect of roadway surrounding rock.

the gob-side roadway did not exceed 130 mm, the maximum deformation was approximately 128 mm for the two sides, and the maximum subsidence of the middle roof was 76 mm. The control effect of surrounding rock is shown in Figure 16. Furthermore, the deformation of the surrounding rock was controllable, and the control effect of the surrounding rock's deformation on the gob-side roadway is obvious.

7. Conclusion

(1) Analyzing the structural characteristics of overburden rock in a gob-side entry with large mining height indicated that the support mode and strength in the driving stage are the crucial guarantees for the gob-side roadway to withstand the influence of subsequent mining.

(2) The surrounding rock failure of the roadway is a process of elasticity-elastoplasticity-plasticity transformation, and it develops from the surface to the interior and eventually to the deep surrounding rock.

(3) The failure mode of the surrounding rock of a gob-side entry with large mining height includes the combination of compression-shear failure, tensile failure, and multiple-shear failure.

(4) According to the field measurement, theoretical analysis, numerical simulation, and the convergence characteristics of surrounding rock after the improvement of support scheme, it can be seen that the mine pressure behavior of gob-side roadway is more severe.

(5) The supporting concepts of maintaining the integrity of the coal pillar, improving the coordination of the system, and using the asymmetric support structure was proposed. The asymmetric support scheme with a prestressed anchor cable as the core component was put forward and was verified by engineering practice.

Data Availability

The data used to support the findings of this study are available from the corresponding author upon request.

Conflicts of Interest

The author declares that there are no conflicts of interest regarding the publication of this paper.

Acknowledgments

This research was financially supported by the Science and Technology Innovation project of Beijing China Coal Mine Engineering Co., Ltd (BMC-ZL-202009), the National Natural Science Foundation of China (no. 51874173), and the Technology Innovation and Entrepreneurship Foundation of CCTEG (no. 2020-2-GJHZ009).

References

[1] K. Terzaghi, "The shearing resistance of saturated soils and the angle between the planes of shear," in *Proceedings of 1st International Conference on Soil Mechanics and Foundation Engineering*, Cambridge, MA, USA, June 1936.

[2] N. R. Barton and E. Grimstad, "Rock mass conditions dictate choice between NMT and NATM," *Tunnels and Tunnelling*, vol. 26, no. 10, pp. 39–42, 1994.

[3] N. Ma, L. Ji, and Z. Zhao, "Distribution of the deviatoric stress field and plastic zone in circular roadway surrounding rock," *Journal of China University of Mining & Technology*, vol. 44, no. 2, pp. 206–213, 2015.

[4] F. L. He, X. M. Wang, D. Q. Zhang et al., "Study on parameters of support for control of roof fall and rib spalling in large fully mechanized top coal caving end face," *Advanced Materials Research*, vol. 616-618, pp. 421–425, 2013.

[5] H. Dulacska, "Dowel action of reinforcement crossing cracks in concrete," *Journal of the American Concrete Institute*, vol. 69, no. 12, pp. 754–757, 1972.

[6] M. V. Ozdogan, H. Yenice, A. Gonen et al., "Optimal support spacing for steel sets: omerler underground coal mine in western Turkey," *International Journal of Geomechanics*, vol. 18, no. 2, pp. 142–145, 2017.

[7] A. Ansell, "Dynamic testing of steel for a new type of energy absorbing rock bolt," *Journal of Constructional Steel Research*, vol. 62, no. 5, pp. 501–512, 2006.

[8] L. St-Pierre, F. P. Hassani, P. H. Radziszewski, and J. Ouellet, "Development of a dynamic model for a cone bolt,"

International Journal of Rock Mechanics and Mining Sciences, vol. 46, no. 1, pp. 107–114, 2009.

[9] F. Charette and M. Plouffe, "Roofex-results of laboratory testing of a new concept of yieldable tendon," *Deep Mining*, vol. 27, no. 7, pp. 395–404, 2007.

[10] C. C. Li, "A new energy-absorbing bolt for rock support in high stress rock masses," *International Journal of Rock Mechanics & Mining Sciences*, vol. 47, no. 3, pp. 396–404, 2010.

[11] C. C. Li and C. Doucet, "Performance of D-bolts under dynamic loading," *Rock Mechanics and Rock Engineering*, vol. 45, no. 2, pp. 193–204, 2012.

[12] M. He, W. Gong, J. Wang et al., "Development of a novel energy-absorbing bolt with extraordinarily large elongation and constant resistance," *International Journal of Rock Mechanics and Mining Sciences*, vol. 67, no. 67, pp. 29–42, 2014.

[13] S. Mahdevari, K. Shahriar, M. Sharifzadeh et al., "Stability prediction of gate roadways in longwall mining using artificial neural networks," *Neural Computing & Applications*, vol. 28, no. 11, pp. 1–19, 2016.

[14] G. Zhang, Z. Wen, S. Liang et al., "Ground response of a gob-side entry in a longwall panel extracting 17m-thick coal seam: a case study," *Rock Mechanics and Rock Engineering*, vol. 53, no. 20, pp. 497–516, 2019.

[15] G. Zhang, F. He, H. Jia, and Y. Lai, "Analysis of gateroad stability in relation to yield pillar size: a case study," *Rock Mechanics and Rock Engineering*, vol. 50, no. 5, pp. 1–16, 2017.

[16] H. Xing, Q. Liu, and Z. Qiao, "Research on large deformation mechanism and control method of deep soft roadway in Zhuji coal mine," *Rock and Soil Mechanics*, vol. 33, no. 3, pp. 827–834, 2012.

[17] M. He, G. Zhang, and Q. Gan, "Stability control of surrounding rocks in deep entry of jiahe coal mine," *Journal of Mining & Safety Engineering*, vol. 24, no. 1, pp. 27–30, 2007.

[18] K. Petr, K. Soucek, S. Lubomir et al., "Long-hole destress blasting for rockburst control during deep underground coal mining," *International Journal of Rock Mechanics and Mining Sciences*, vol. 61, pp. 141–153, 2013.

[19] L. Yuan, J. Xue, and Q. Liu, "Surrounding rock stability control theory and support technique in deep rock roadway for coal mine," *Journal of China Coal Society*, vol. 36, no. 4, pp. 535–543, 2011.

[20] D. Roy, J. Howell, R. Boyd et al., "High-resolution sequence-stratigraphic correlation between shallow-marine and terrestrial strata: examples from the sunnyside member of the cretaceous blackhawk formation, book cliffs, eastern Utah," *American Association of Petroleum Geologists Bulletin*, vol. 90, no. 7, pp. 1121–1140, 2006.

[21] Y. L. Tan, F. H. Yu, J. G. Ning, and T. B. Zhao, "Design and construction of entry retaining wall along a gob side under hard roof stratum," *International Journal of Rock Mechanics and Mining Sciences*, vol. 77, no. 77, pp. 115–121, 2015.

[22] P. Konicek, K. Soucek, L. Stas, and R. Singh, "Long-hole destress blasting for rockburst control during deep underground coal mining," *International Journal of Rock Mechanics and Mining Sciences*, vol. 61, pp. 141–153, 2013.

[23] Z. Y. Zhang, H. Shimada, D. Y. Qian et al., "Application of the retained gob-side gateroad in a deep underground coalmine," *International Journal of Mining Reclamation and Environment*, vol. 30, no. 5, pp. 71–379, 2015.

[24] M. Qian, "A study of the behavior of overlying strata in long wall mining and its application to strata control," *Developments in Geotechnical Engineering*, vol. 32, pp. 13–17, 1982.

[25] M. G. Qian, F. L. He, and X. X. Miao, "The system of strata control around longwall face in China," *Mining Science and Technology*, vol. 79-80, pp. 15–18, 1996.

[26] J.-j. Shi, N.-j. Ma, P. Zhan, and D.-l. Zhang, "Study on the material character steel big-end bolt," *Journal of Coal Science and Engineering (China)*, vol. 14, no. 4, pp. 616–620, 2008.

[27] F. Xie, M. Xing, F. He et al., "Asymmetric reinforcement field test of large section roadway driving along next goaf in longwall top-coal mining," *Electronic Journal of Geotechnical Engineering*, vol. 21, no. 5, pp. 1909–1920, 2016.

[28] O. T. Bruhns, H. Xiao, and A. Meyers, "A self-consistent Eulerian rate type model for finite deformation elastoplasticity with isotropic damage," *International Journal of Solids and Structures*, vol. 38, no. 4, pp. 657–683, 2001.

[29] H. Wang, B. A. Poulsen, B. Shen, S. Xue, and Y. Jiang, "The influence of roadway backfill on the coal pillar strength by numericalinvestigation," *International Journal of Rock Mechanics and Mining Sciences*, vol. 48, no. 3, pp. 443–450, 2011.

[30] W. Gao, "Study on the width of the non-elastic zone in inclined coal pillar for strip mining," *International Journal of Rock Mechanics & Mining Sciences*, vol. 72, no. 5, pp. 304–310, 2014.

[31] K. Chen, "Research on failure evolution and control mechanism of surrounding rock of deep roadways and its application," *China university of mine and technology press*, vol. 2009, Article ID 1835381, 14 pages, 2009.

[32] W. J. Gale and R. L. Blackwood, "Stress distributions and rock failure around coal mine roadways," *International Journal of Rock Mechanics and Mining Sciences & Geomechanics Abstracts*, vol. 24, no. 3, pp. 165–173, 1987.

[33] W. He, F. He, D. Chen et al., "Pillar width and surrounding rock control of gob-side roadway with mechanical caved mining in extra-thick coal seams under hard-thick main roof," *Journal of Mining& Safety Engineering*, vol. 37, no. 2, pp. 349–358+365, 2020.

[34] H. Qi and J. Yu, "Rationality and comprehensive unloading technology of deep high stress section coal pillars," *Journal of China Coal Society*, vol. 43, no. 12, pp. 3257–3264, 2018.

[35] J. Guo, W. Wang, F. He et al., "Main roof break structure and surrounding stability analysis in gob-side entry with fully-mechanized caving mining," *Journal of Mining & Safety Engineering*, vol. 36, no. 3, pp. 446–454+464, 2019.

[36] F. Xie, F. He, S. Yin et al., "Study on asymmetric control of large section gob-side coal entry influenced by strong mining," *Journal of Mining & Safety Engineering*, vol. 33, no. 6, pp. 999–1007, 2016.

[37] W. Wang, C. Yuan, W. Yu et al., "Stability control method of surrounding rock in deep roadway with large deformation," *Journal of China Coal Society*, vol. 41, no. 12, pp. 2921–2931, 2016.

[38] Y. Cheng, Y. Ma, Z. Hu et al., "Mechanism and key technologies of preventing rock burst by outward staggered entries arrangment in fully-mechanized caving mining face," *Journal of China Coal Society*, vol. 41, no. 3, pp. 564–570, 2016.